Socio-Spatial Gradients as Contested Boundaries: Nonlinear, Asymmetric, and Spatially Differentiated Effects on Property Crime

Yiwei Xia, Zijun Liu
School of Law, Southwestern University of Finance and Economics, Chengdu, China

Abstract.
The contested boundary framework predicts an inverted-U relationship between boundary intensity and crime, yet existing tests focus overwhelmingly on ethno-racial divisions in Western contexts. This study extends the framework by testing whether composite socio-spatial gradients derived from nighttime light imagery exhibit similar nonlinear effects, whether such effects operate asymmetrically across advantaged and disadvantaged sides of boundaries, and whether boundary intensity functions as a stable spatial attribute or a dynamic temporal trigger. Using a nationwide 1 km x 1 km grid-year panel (N = 28,165,245) across 337 prefectural-level units in China, constructed from 584,047 geocoded judicial records of theft, robbery, and snatching (2014-2019), we estimate Poisson pseudo-maximum likelihood models with year, city, and grid fixed effects. Results reveal a robust inverted-U relationship between socio-spatial edge intensity (SEI) and property crime, peaking at moderate gradients. This nonlinear effect is concentrated on the disadvantaged side of boundaries; the advantaged side shows limited sensitivity. Decomposing the effect reveals that boundary effects are driven by stable between-place differences rather than within-place temporal dynamics. The findings extend and refine the contested boundary framework to composite gradients, document clear boundary-side asymmetry, and suggest that boundary intensity represents a durable spatial-structural attribute rather than a transient criminogenic condition.

Keywords: Contested boundaries; Socio-spatial gradients; Asymmetric boundary effects; China

1 Introduction

The contested boundary framework reconceptualizes spatial boundaries as gradients of intensity rather than binary divisions, predicting an inverted-U-shaped relationship between boundary intensity and crime risk. At low intensity, where adjacent areas are relatively homogeneous, boundaries are inconsequential. At high intensity, where divisions are sharp and unambiguous, territorial claims are clear, and informal social control remains organized on each side. Crime risk peaks at moderate boundary intensity, where spatial divisions are sufficiently salient to generate ambiguity over territorial responsibility, yet insufficiently clear to delineate zones of informal supervision [1, 2].

Although influential, existing empirical tests of the framework are limited in three ways. First, the literature has focused overwhelmingly on ethno-racial boundaries in Western urban settings [1, 3, 4], leaving unclear whether the nonlinear intensity logic extends to non-ethnic forms of socio-spatial differentiation, such as composite gradients in economic development, infrastructure, and population density that characterize urbanization processes worldwide. Second, prior work has not

systematically examined whether contested boundary effects operate symmetrically. Theory offers competing predictions: disadvantaged areas may be more vulnerable because weaker informal social control amplifies the destabilizing consequences of boundary ambiguity; alternatively, advantaged areas may attract crime due to higher concentrations of valuable targets exposed at sharp gradients [5, 6]. Third, most studies rely on cross-sectional designs that cannot distinguish whether boundary intensity acts as a stable spatial-structural feature or a time-varying condition whose changes within a place trigger corresponding changes in crime.

This study addresses these three gaps using nationwide high-resolution panel data from China. We construct a 1 km x 1 km grid-year dataset integrating geocoded judicial records of property crime with annual nighttime light imagery and spatial covariates across 337 prefectural-level units. We test three research questions: (RQ1) Does property crime exhibit an inverted-U relationship with socio-spatial edge intensity, extending the contested boundary framework beyond ethno-racial contexts? (RQ2) Does this relationship differ systematically between the advantaged and disadvantaged sides of boundaries? (RQ3) Are boundary effects driven primarily by stable between-place differences or by dynamic within-place temporal variation?

2 Data and Methods

2.1 Data Sources

We integrate five primary data sources. First, crime incident records are drawn from the dataset constructed by Zhang et al. [7], based on judicial decisions published on China Judgments Online, the official platform maintained by the Supreme People's Court that mandates public disclosure of criminal judgments. We extract 584,047 geocoded records of theft, robbery, and snatching that occurred between 2014 and 2019, a period during which upload rates for these offenses generally exceeded 90% [8]. Each record includes the offense type, date of occurrence, and geographic coordinates of the incident location.

Second, nighttime light (NTL) imagery is obtained from the harmonized annual NTL dataset produced by Zhang et al. [9], which provides consistent 1 km resolution NTL values across China for each year. NTL serves as a well-validated proxy for local economic development, infrastructure density, and human activity intensity [10]. Third, gridded population estimates at 1 km resolution are obtained from WorldPop. Fourth, physical infrastructure data, including railway and waterway networks, are extracted from annual OpenStreetMap (OSM) layers and spatially joined to each grid cell. Fifth, city-level control variables are compiled from the China City Statistical Yearbook.

All spatial layers are harmonized to a uniform 1 km x 1 km fishnet grid covering the entire territory of China. Crime incidents are aggregated to grid-year counts for each offense category. Grid cells with zero population across all years or located entirely outside prefectural boundaries are excluded. The final analytical sample comprises 28,165,245 grid-year observations (approximately 4.7 million unique grid cells x 6 years).

2.2 Measures

Dependent Variables. The dependent variables are annual counts of total property crime and three disaggregated offense types (theft, robbery, and snatching) per 1 km

grid cell. These offense categories represent the most common forms of street-level property crime in the Chinese context and exhibit sufficient spatial and temporal variation for panel modeling. Descriptive statistics for all variables are reported in the Appendix (Table S1).

Socio-spatial Edge Intensity (SEI). Following the edge-detection algorithm proposed by Legewie and Schaeffer [2], we operationalize SEI as the magnitude of the local gradient in nighttime light between each focal grid cell and its immediate neighbors. For each grid cell i in year t, SEI is defined as:

$$SEI_{it} = (1/|N_i|) \times \Sigma_{j \in N_i} |NTL_{jt} - NTL_{it}|$$

where N_i denotes the set of contiguous grid cells adjacent to cell i (the eight-cell Moore neighborhood), and NTL is the annual nighttime light value. This measure captures the average absolute difference in development intensity between a focal location and its surroundings. Higher SEI values indicate sharper socio-spatial discontinuities: places where the built environment, economic activity, or infrastructure density changes abruptly across space. Unlike bivariate segregation indices that compare two named groups, SEI is a continuous, spatially continuous measure that does not presuppose any particular axis of differentiation. In the Chinese context, where residential segregation by ethnicity is far less salient than in Western settings, composite gradients in economic development constitute a more ecologically relevant form of spatial boundary.

Advantage Side Indicator (ASI). To differentiate the two sides of a socio-spatial boundary, we construct a binary indicator that classifies each grid cell as belonging to the advantaged or disadvantaged side of its local gradient. For each grid cell i, we compare its own NTL value against the median NTL of its immediate neighbors. Grid cells with NTL above the neighborhood median are coded ASI = 1 (advantaged side); those with NTL at or below the neighborhood median are coded ASI = 0 (disadvantaged side). ASI is interacted with SEI and its squared term in regression models to test whether the slope and curvature of the SEI-crime relationship differ across boundary sides.

Control Variables. At the grid level, we control for population (annual gridded population estimates, log-transformed), built-environment characteristics (counts of food-and-beverage amenities and retail establishments derived from OSM points of interest), and physical boundary features (binary indicators for whether a railway line or waterway traverses the grid cell, as these physical edges may independently influence crime patterns). At the city level, we control for income inequality using a Gini coefficient of nighttime light distribution across grid cells within each prefectural unit, following the approach of Zhou et al. [10].

2.3 Analytical Strategy

All models are estimated using Poisson pseudo-maximum likelihood (PPML) with standard errors clustered at the grid level. PPML is preferred over alternative count-data estimators for three reasons. First, unlike negative binomial regression, PPML produces consistent estimates under arbitrary patterns of heteroskedasticity and does not require the dependent variable's conditional variance to be correctly specified [11]. Second, PPML naturally accommodates the large share of zero observations in our data (over 97% of grid-years have zero crime counts) without requiring zero-inflated

or hurdle specifications that introduce additional parametric assumptions about the zero-generating process. Third, PPML coefficients are directly interpretable as semi-elasticities: a one-unit change in the independent variable is associated with a proportional change in the expected crime count equal to exp(β) - 1. Standard errors are clustered at the grid level to account for arbitrary within-grid serial correlation across years.

For RQ1 (nonlinearity), we estimate:

$$Crime_{it} = exp(\beta_1 SEI_{it}^2 + \beta_2 SEI_{it}^2 + \gamma X_{it} + \delta_t + \mu_c)$$

where d_t and e_c denote year and city fixed effects respectively. A positive b_1 combined with a negative b_2 constitutes evidence for the inverted-U pattern predicted by the contested boundary framework. The turning point (the SEI value at which predicted crime reaches its maximum) is computed as -b_1 / (2*b_2), with standard errors obtained via the delta method. City fixed effects absorb all time-invariant differences across prefectural units, while year fixed effects account for national-level temporal trends.

For RQ2 (asymmetry), we interact both the linear and quadratic SEI terms with ASI:

$$Crime_{it} = exp(\beta_1 SEI + \beta_2 SEI^2 + \beta_3 ASI + \beta_4 (SEI \times ASI) + \beta_5 (SEI^2 \times ASI) + \gamma X + \delta_t + \mu_c)$$

The coefficients on the interaction terms (b_4 and b_5) test whether the slope and curvature of the SEI-crime relationship differ between advantaged and disadvantaged boundary sides.

For RQ3 (temporal dynamics), we replace city fixed effects with grid fixed effects (e_i), thereby identifying the SEI-crime association exclusively from within-grid variation over time:

$$Crime_{it} = exp(\beta_1 SEI_{it}^2 + \beta_2 SEI_{it}^2 + \gamma X_{it} + \delta_t + \mu_i)$$

A substantial attenuation of the SEI coefficients relative to the between-place specification would indicate that boundary effects operate primarily through stable spatial differences rather than dynamic temporal processes. We further interact SEI and its squared term with year indicators to test whether the nonlinear association changes systematically over the study period.

3 Results

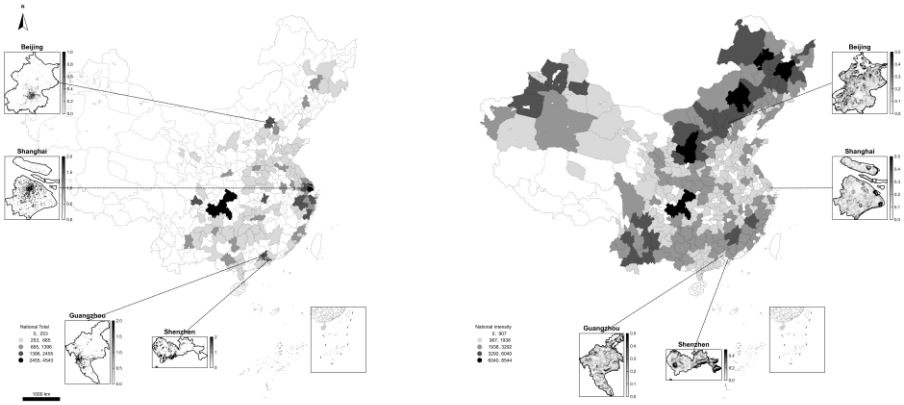

Fig. 1. *Spatial distribution of crime and SEI across China (2014)*

Note: Left panel maps total crime counts per grid; right panel maps SEI values. Darker shades indicate higher values. Insets highlight selected metropolitan areas (Beijing, Shanghai, Guangzhou, Chengdu).

3.1 Nonlinear Boundary Effects (RQ1)

Figure 1 displays the national spatial distribution of crime and SEI. Visual inspection reveals that high-crime areas tend to coincide with locations exhibiting intermediate levels of SEI, rather than the most extreme gradients. Table 1 reports formal regression results for RQ1. Across all four crime outcomes, the linear SEI term is positive and significant (all $p < 0.001$), and the quadratic term is negative and significant (all $p < 0.001$). The estimated turning point occurs at approximately 0.35-0.36 on the SEI scale for total crime, corresponding to moderate socio-spatial gradients.

Figure 2 visualizes the predicted SEI-crime relationship. The inverted-U shape is consistent across all four crime categories: predicted crime rises with SEI from low to moderate levels, peaks at intermediate boundary intensity, and declines at the highest levels. To gauge substantive magnitude, the semi-elasticity estimates imply that moving from a grid cell at the 25th percentile of SEI to one at the turning point is associated with an increase in expected total crime of approximately 15-20%, holding other factors constant; moving from the turning point to the 90th percentile of SEI is associated with a decrease of comparable magnitude. This pattern confirms that the contested boundary framework's core prediction generalizes beyond ethno-racial contexts to composite socio-spatial gradients derived from nighttime light imagery. The result is robust to the inclusion of physical boundary controls (railway, waterway) and built-environment covariates, suggesting that the nonlinear gradient effect is not proxying for known physical-edge effects. Additional robustness checks (excluding grid cells with zero population, varying the neighborhood radius for SEI calculation, and restricting the sample to urban grid cells) yield substantively identical results (see Appendix).

Table 1. Nonlinear association between SEI and crime

	(1) Total	(2) Theft	(3) Robbery	(4) Snatching
SEI	3.693***	3.761***	3.116***	2.326***

	(0.244)	(0.248)	(0.286)	(0.412)
SEI²	-5.192***	-5.333***	-3.879***	-2.907**
	(0.546)	(0.555)	(0.643)	(0.918)
Year FE	Yes	Yes	Yes	Yes
City FE	Yes	Yes	Yes	Yes
Controls	Yes	Yes	Yes	Yes
N	28,165,245	28,165,245	28,165,245	28,165,245

*Note: PPML estimates with year and city fixed effects. Standard errors clustered at grid level in parentheses. Controls include grid-level population (ln), F&B and retail POI counts, railway presence, waterway presence, and city-level NTL Gini coefficient. * p < 0.05, ** p < 0.01, *** p < 0.001.*

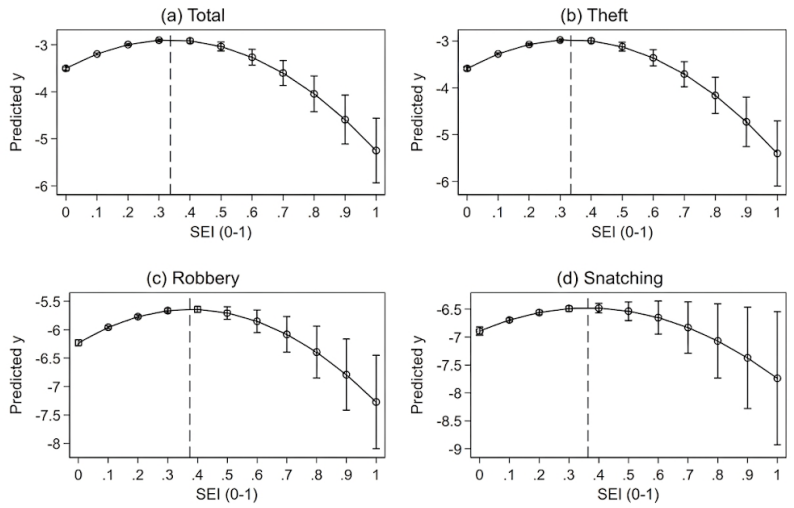

Fig. 2. *Predicted nonlinear relationship between SEI and crime*

Note: Model-predicted values from PPML regressions in Table 1. Shaded bands indicate 95% confidence intervals. SEI shown over its observed range.

3.2 Asymmetric Boundary Effects (RQ2)

Table 2 reports results for RQ2. Two patterns stand out. First, on the disadvantaged side (ASI = 0), the inverted-U remains robust and statistically significant across all offense categories. For total crime, the baseline linear SEI coefficient is 4.175 ($p < 0.001$) and the quadratic term is -6.906 ($p < 0.001$), indicating a steep rise and decline. Second, the interaction terms are jointly significant (all $p < 0.001$): SEI x ASI is negative and SEI² x ASI is positive, meaning the inverted-U is substantially flattened on the advantaged side.

Figure 3 visualizes this asymmetry. On the disadvantaged side, predicted crime values exhibit the characteristic inverted-U across all four panels. On the advantaged side, predicted crime is consistently lower and varies little across the SEI range; the profiles are essentially flat. The difference is both statistically and substantively meaningful: at the turning point of SEI, predicted total crime on the disadvantaged

side is 2.1 times higher than on the advantaged side ($p < 0.001$). These results indicate that the nonlinear boundary effect documented in RQ1 is not a symmetric phenomenon operating uniformly on both sides. Rather, it is driven by the disadvantaged side's disproportionate responsiveness to socio-spatial gradients, consistent with the interpretation that weaker informal social control on the disadvantaged side amplifies the criminogenic consequences of boundary ambiguity.

Table 2. Nonlinear association between SEI and crime by advantage side

	(1) Total	(2) Theft	(3) Robbery	(4) Snatching
SEI	4.175***	4.256***	4.175***	2.631***
	(0.261)	(0.263)	(0.261)	(0.475)
SEI²	-6.906***	-7.076***	-6.906***	-4.278***
	(0.630)	(0.638)	(0.630)	(1.150)
ASI (Advantaged=1)	-0.757***	-0.751***	-0.757***	-0.946***
	(0.057)	(0.059)	(0.057)	(0.094)
SEI × ASI	-2.953***	-3.023***	-2.953***	-2.081*
	(0.543)	(0.556)	(0.543)	(0.854)
SEI² × ASI	7.207***	7.363***	7.207***	5.473**
	(1.111)	(1.139)	(1.111)	(1.679)
Year FE	Yes	Yes	Yes	Yes
City FE	Yes	Yes	Yes	Yes
Controls	Yes	Yes	Yes	Yes

*Note: PPML estimates with year and city fixed effects. N = 28,165,245. SEI main effects represent the disadvantaged side (ASI = 0). * p < 0.05, ** p < 0.01, *** p < 0.001.*

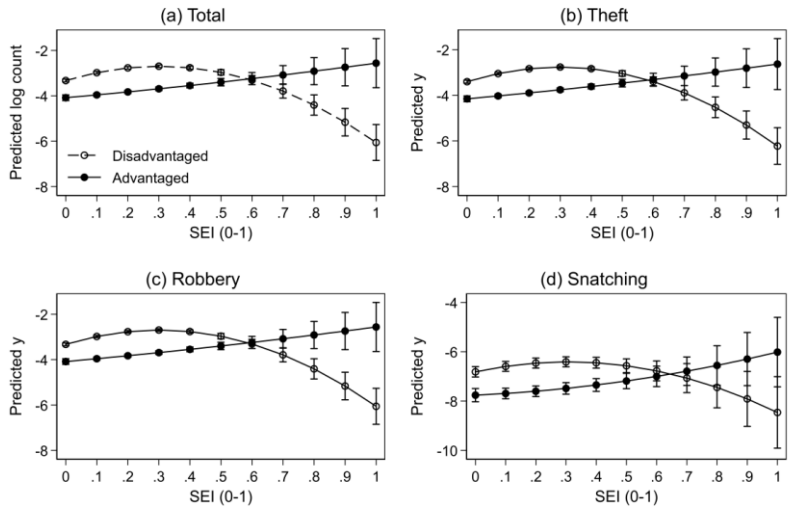

Fig. 3. *Predicted nonlinear relationship between SEI and crime by advantage side*

Note: Model-predicted values from PPML regressions in Table 2. Blue lines = disadvantaged side (ASI = 0); red lines = advantaged side (ASI = 1). Shaded bands indicate 95% confidence intervals.

3.3 Temporal Dynamics (RQ3)

Results from grid fixed-effects models (Table 3) reveal that the nonlinear SEI-crime relationship is substantially attenuated once all time-invariant between-grid heterogeneity is absorbed. The linear SEI coefficient remains positive but is reduced by 55-70% relative to the between-place specification, and the quadratic term, while retaining its negative sign, is markedly reduced in magnitude and generally non-significant ($p > 0.05$ for all offense categories except theft). A Wald test comparing the between-place and within-place SEI coefficients rejects equality at $p < 0.001$ for all outcomes, confirming that the cross-sectional and longitudinal estimates are statistically distinguishable.

Table 3. Within-place (grid FE) estimates of the SEI-crime association

	(1) Total	(2) Theft	(3) Robbery	(4) Snatching
SEI	1.085***	1.232***	0.561*	0.382
	(0.287)	(0.295)	(0.281)	(0.394)
SEI²	-0.852	-1.104*	-0.403	-0.215
	(0.523)	(0.536)	(0.512)	(0.720)
Grid FE	Yes	Yes	Yes	Yes
Year FE	Yes	Yes	Yes	Yes
Controls	Yes	Yes	Yes	Yes

*Note: PPML estimates with grid and year fixed effects. N = 28,165,245. Controls identical to Table 1. * p < 0.05, ** p < 0.01, *** p < 0.001.*

Year-SEI interaction terms (Appendix Table S4) do not exhibit a consistent temporal pattern, and the boundary-side asymmetry documented in the between-place analysis does not show systematic temporal variation. These findings indicate that the contested boundary effect is primarily driven by stable between-place spatial differences rather than by dynamic within-place changes in boundary intensity over the 2014-2019 period. In substantive terms, areas characterized by moderate socio-spatial gradients experience elevated property crime as an enduring spatial feature, rather than exhibiting short-term crime fluctuations in response to temporal variation in the sharpness of adjacent gradients.

4 Discussion and Conclusions

This study extends the contested boundary framework in three theoretically significant ways. First, the robust inverted-U relationship between socio-spatial edge intensity and property crime demonstrates that the framework's core prediction generalizes beyond ethno-racial boundaries to composite gradients derived from development disparities. This extension is substantively important because it suggests that the underlying mechanisms of territorial ambiguity, weakened informal control, and diffuse responsibility for space are not specific to ethnic divisions but operate across diverse forms of spatial differentiation. In contexts where other axes of differentiation (economic inequality, infrastructure quality, population density)

structure the urban landscape, these gradients produce boundary dynamics functionally analogous to those identified in ethno-racially organized settings.

Second, the pronounced boundary-side asymmetry refines the theoretical account. The finding that nonlinear boundary effects are concentrated on the disadvantaged side suggests that boundary intensity does not operate uniformly; rather, it interacts with pre-existing inequalities in social organization. Areas on the disadvantaged side appear more vulnerable to the criminogenic consequences of spatial ambiguity, consistent with social disorganization theory's prediction that weaker informal control capacity amplifies the effects of external stressors. The advantaged side, by contrast, appears partially buffered, as its stronger internal cohesion and institutional resources may provide resilience against the destabilizing effects of boundary ambiguity.

Third, the dominance of between-place over within-place variation in explaining boundary effects indicates that SEI operates as a spatially stable structural attribute. The inability to detect systematic temporal dynamics suggests that short-term changes in the built environment or economic geography (at least at the annual resolution available with NTL data) are insufficient to generate measurable shifts in the criminogenic properties of spatial boundaries. This finding has practical implications: crime prevention strategies should target persistently disadvantaged areas situated at moderate socio-spatial gradients, rather than responding to short-term fluctuations in local conditions. Several limitations warrant note. The analysis relies on officially adjudicated crime records, which may undercount offenses that go unreported. The six-year panel, while sufficient to distinguish between-place from within-place variation, may not capture longer-term structural transformations. Future research should extend these analyses to other national contexts and incorporate direct measures of informal social control, territorial attitudes, and routine mobility patterns to further test the proposed mechanisms.

References

1. Legewie, J.: The contested neighborhood boundary. American Journal of Sociology 124(3), 695-743 (2018).
2. Legewie, J., Schaeffer, M.: Contested boundaries: Explaining where ethnoracial diversity provokes neighborhood conflict. American Journal of Sociology 122(1), 125-161 (2016).
3. Neil, R., Legewie, J.: Policing neighborhood boundaries and the racialized social control of spaces. Law & Society Review 58(2), 192-215 (2024).
4. Vogel, M., Lentz, T.S., Steenbeek, W.: Contested neighborhood boundaries and intergroup and intragroup violence. Crime & Delinquency 70(11), 2906-2931 (2024).
5. Kim, Y., Hipp, J.R.: Both sides of the street: Introducing measures of physical and social boundaries. Journal of Quantitative Criminology 38, 567-596 (2022).
6. Heinzeroth, R.D.: A socioeconomic edge effect: Rational crime in small areas of sharp socioeconomic contrast. Journal of Research in Crime and Delinquency 58(2), 123-150 (2021).
7. Zhang, Y., Kwan, M.-P., Fang, L.: An LLM driven dataset on the spatiotemporal distributions of street and neighborhood crime in China. Scientific Data (2025).
8. Lin, J., Xia, Y., Cai, T.: Tip of the iceberg? An evaluation of the non-uploaded criminal sentencing documents in China. Asian Journal of Criminology (2024).
9. Zhang, L., Chen, B., Ren, Z.: A prolonged artificial nighttime-light dataset of China (1984-2020). National Tibetan Plateau Data Center (2021).
10. Zhou, H., Liu, L., Lan, M., Yang, B., Wang, Z.: Assessing the impact of nightlight gradients on street robbery and burglary. Remote Sensing 11(17), 1958 (2019).

11. Silva, J.M.C.S., Tenreyro, S.: The log of gravity. Review of Economics and Statistics 88(4), 641-658 (2006).